ChemPubSoc Europe

DOI: 10.1002/ejic.201901223

EurJIC European Journal of Inorganic Chemistry

Full Paper

Bioisosters

Higher Carbon Analogues of 1,4-Dihydropyridines as Potent TGFβ/Smad Inhibitors

Eva R. Barth,[a] Daniel Längle,[b][‡] Fabian Wesseler,[b][‡] Christopher Golz,[a] Anna Krupp,[a] Dennis Schade,[b][‡] and Carsten Strohmann*[a]

Abstract: The C to Si and Ge exchange in bioactive compounds has often led to positive changes in the molecular properties, whereby Ge analogues are underrepresented. This is only possible at tetrahedral positions, and it is necessary for the analogue building blocks to withstand the synthetic conditions. Here, we present the synthesis of Si and Ge analogues of a TGFβ inhibiting 1,4-dihydropyridine, which has a tetrahedral carbon in an important position for its activity. The molecular properties are compared by the discussion of the single X-ray crystal structures and the electrostatic potential on the molecule surface which could play a role in the target interaction. Biological activities show that the C to Si and Ge exchange goes with full preservation of the potency, thus representing good starting points to modify physicochemical features and pharmacokinetics of these TGFβ inhibitors.

Introduction

Many processes in the human body are controlled by ligand-receptor interactions on the surface of cells, which then activate or inhibit specific signalling pathways to produce a biochemical response. Pathways involved in the onset and progression of diseases such as cancer, diabetes and cardiovascular diseases are of particular interest for medical research. In this context, the TGF/Smad (Transforming Growth Factor) signalling pathway often plays a key role as it is involved in cell differentiation, cell migration and proliferation.[1] To date, several small molecule TGFβ inhibitors have been described which mostly target the receptor kinase domains.[2] However, using a phenotypic screening in stem cells, the substance class of 1,4-dihydropyridines (DHPs) was identified as TGFβ inhibitors.[3] Importantly, these compounds inhibit TGFβ signaling via stimulation of proteasomal degradation of the type II TGFβ receptor. Following our initial studies on the structure activity relationships of the identified hit compound **1** (see Figure 1),[3,4] we substantially explored the structure activity relationships for this unique class of TGFβ inhibitors in a seminal series of reports.[5] Among several SAR-optimized derivatives, 4′-(*tert*-butyl) DHP analogue **2** (see Figure 1) was highly potent (i.e., IC_{50} = 0.28 μM).

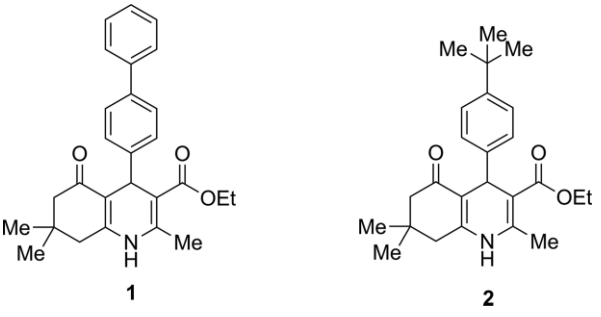

Figure 1. Chemical structures of the 1,4-dihydropyridine-class of TGFβ inhibitors, with an early hit compound **1** and the potent 4′-*tert*-butyl analogue **2**.[6]

Here, we report on interesting derivatives of **2** containing the higher carbon analogues silicon and germanium at the 4′ position. We investigated the influence of these elements to the molecular structure, its electronic properties (especially the resulting partial charges) that are crucial for the target interaction, as well as their biological activity as TGFβ inhibitors. In addition to fine-tuning of the DHP's physicochemical features by the altered electronegativity, the possibility of introducing further interesting element properties into the compounds was also explored. In the past, silicon analogues of active substances have often shown positive effects such as increased lipophilicity or blocking of certain metabolic pathways.[7] In comparison to C/Si isosterism there are only a few reports on Ge analogues

[a] *Department of Inorganic Chemistry, Faculty of Chemistry and Chemical Biology, Dortmund University of Technology, Otto-Hahn-Straße 6/6a, 44227 Dortmund, Germany*
E-mail: carsten.strohmann@tu-dortmund.de
http://www.carbanion.de
[b] *Department of Chemistry and Chemical Biology, Technical University Dortmund, Otto-Hahn-Str. 4, 44227 Dortmund, Germany*
[‡] Current address:
Department of Pharmaceutical and Medicinal Chemistry, Christian-Albrechts-University Kiel, Gutenbergstr. 76, 24118 Kiel, Germany
E-mail: schade@pharmazie.uni-kiel.de
https://www.pharmazie.uni-kiel.de/de/pharmazeutische-chemie/prof-dr-dennis-schade

Supporting information and ORCID(s) from the author(s) for this article are available on the WWW under https://doi.org/10.1002/ejic.201901223.

for which increased lipophilicity and low toxicity were achieved.[8] Here it seems to be interesting to insert germanium so that the follow-up studies on metabolism and the detection of degradation products via mass spectrometry can be facilitated due to its characteristic isotope pattern.[8f]

Results and Discussion

To prepare the *b*-annelated 1,4-dihydropyridines, the general one pot Hantzsch concept was used. As shown in Scheme 1, the silicon and germanium containing benzaldehyde derivatives **5a** and **5b** were prepared as building blocks in two steps starting from 1,4-dibromobenzene and then subjected to the multicomponent reaction to furnish the desired 1,4-dihydropyridine compounds **6a**, **6b** and **2**, respectively.

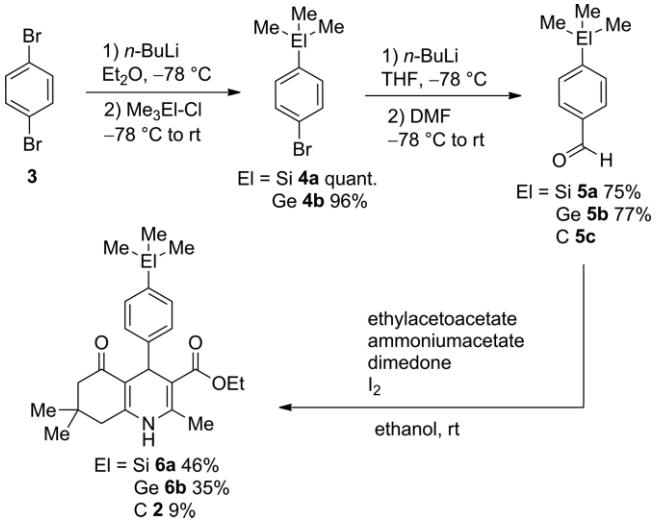

Scheme 1. Synthesis of the 4'-(*tert*-butyl) bioisosteric 1,4-dihydropyridines **6a**, **6b**, and **2**.

After purifying of the DHP compounds via column chromatography, the resulting solid substances were crystallized from ethanol to be used for single-crystal X-ray crystallography. The elementary cell of all three crystal structures contains both enantiomers because the synthesis was racemic. However, since they only differ in the absolute configuration, the discussion of the structures is limited to the (*R*)-enantiomer. In Figure 2, the molecular structure of the carbon DHP compound **2** is shown.

The bond lengths and angles of the *tert*-butyl group correspond to the typical values for C–C single bonds.[7] The phenyl ring is also an ordinary aromatic sp^2 system. Two typical structural features for 1,4-DHPs can also be observed: the flattened boat conformation of the annelated ring system, and the pseudo axial position of the substituent at C40, which is thus almost perpendicular to the ring plane.[5] The angle (N2–C40–C41 107°) here is even steeper than the corresponding angle in the biphenyl derivative **1** (118°).[5] The ethyl ester linked to C29 is also arranged in this plane. In addition, the corresponding ethyl group is present in a disorder caused by the two *cis* and *trans* rotation isomers of C26 related to C28.

Crystals were also obtained for the corresponding silicon compound **6a**, the structure of which is shown in Figure 3.

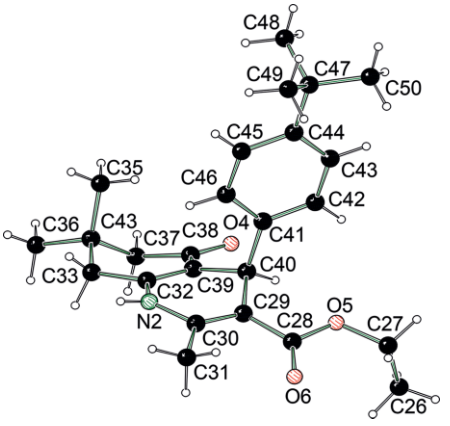

Figure 2. Crystal structure of C-DHP **2**. The compound crystallizes from ethanol in the space group $P2_1/c$ as colorless blocks. Selected bond lengths [Å], angles [°] and torsion angles [°]: C44–C47 1.533(3), C47–C48 1.535(4), C47–C49 1.537(4), C47–C50 1.531(4), C41–C42 1.388(3), C41–C46 1.396(3), C43–C44 1.390(3), C44–C45 1.399(3), C42–C43 1.389(3),C45–C46 1.381(3), C41–C42–C43 121.4(2), C41–C42–C43–C44 –0.5(4), C29–C40–C41–C46 –82.1(3), O5–C28–C29–C30 –170.5(2).

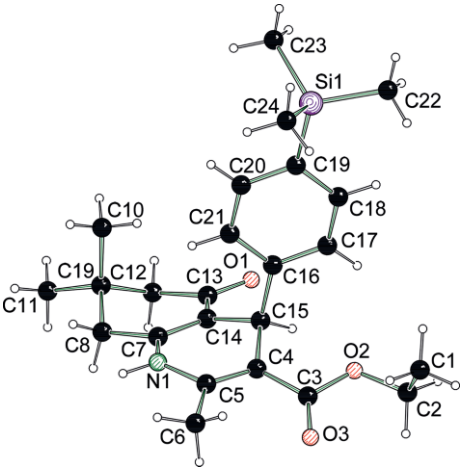

Figure 3. Crystal Structure of Si-DHP **6a**. The compound crystallizes from ethanol in the space group $P2_1/c$ as colorless blocks. Selected bond lengths [Å], angles [°] and torsion angles [°]: Si1–C19 1.8751(15), Si1–C22 1.8599(18), Si1–C23 1.8661(18), Si1–C24 1.8562(19), C16–C17 1.389(2), C16–C21 1.394(2), C17–C18 1.389(2), C18–C19 1.394(2), C19–C20 1.402(2), C20–C21 1.388(2), C18–C17–C16 120.9(1), C16–C17–C18–C19 –0.6(2), C4–C15–C16–C21 –83.4(2), O2–C3–C4–C5 –171.6(1), C3–O2–C2–C1 –79.6(2).

The Si–C distances within the trimethylsilyl group are in the range of 1.8562(19) (Si1–C24) and 1.8661(18) Å (Si1–C23), which, like the distance to the phenyl group [1.8751(15) Å (Si1–C19)], corresponds to typical values of Si–C single bonds.[9a] The angle between the DHP plane and the substituent at position 4 amounts to 106° (N1–C15–C16). The disorder of the ethyl ester group here leads to an almost vertical arrangement of C1 in relation to the ring plane. The other structural characteristics are the same as those of the C-DHP compound described above.

At last, the molecular structure of germanium compound **6b** was determined, which is shown in Figure 4.

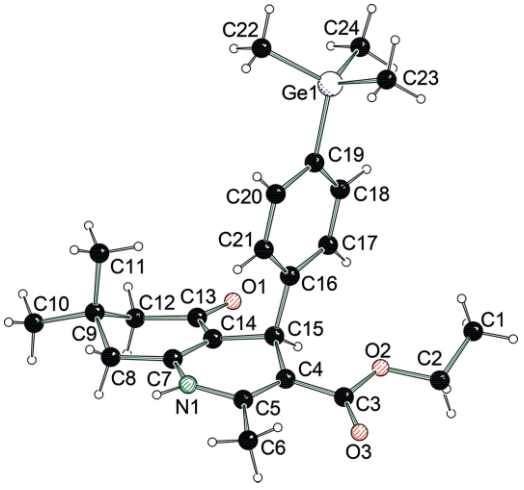

Figure 4. Crystal structure of Ge-DHP **6b**. The compound crystallizes from ethanol in the space group P_{bca} as colorless blocks. Selected bond lenghts [Å], angles [°] and torsion angles [°]: Ge1–C19 1.955(3), Ge1–C22 1.936(4), Ge1–C23 1.945(4), Ge1–C24 1.957(4), C16–C17 1.386(4), C16–C21 1.395(4), C17–C18 1.388(4), C18–C19 1.385(4), C19–C20 1.399(4), C20–C21 1.378(4), C16–C17–C18 121.2(3), C16–C17–C18–C19 –0.1(5), C4–C15–C16–C21 –61.0(3), O2–C3–C4–C5 –174.1(3).

The general structural characteristics of the germanium DHP compound correspond to the lighter homologues. The Ge–C distances within the trimethylgermyl group are in the range of 1.936(4) (Ge1–C22) and 1.957(4) Å (Ge1–C24), which, as well as the distance to the phenyl group [1.955(3) Å (Ge1–C19)] corresponds to typical values of Ge–C single bonds.[9] The angle between the DHP plane and the substituent at position 4 is slightly flattened to 114° (N1–C15–C16) and therefore more similar to **1**. The crystal contained a solvent molecule which, however, was disordered. A cavity was found which matched the volume and electron density of ethanol and was treated with a solvent mask. The germanium DHP structure differs from the silicon and carbon structure in the arrangement of the aromatic plane relative to the vertical center plane of the dihydropyridine ring. However, these are probably packing effects, since germanium compound also crystallizes in another space group and under inclusion of a solvent molecule.

On the basis of quantum chemical calculations on the B3LYP/6-31+G(d) level a free geometry optimization of the three DHP derivatives was carried out. The Conolly surfaces with a sample radius of 1.4 Å were created and assigned with the electrostatic potential to detect the areas of the molecules that are able to interact with the target protein. The results are shown in Figure 5.

The views of the molecule surfaces show two aspects that were expected due to the crystal structures and the different electronegativities of the elements: on the one hand, the increasing steric demand in the area of the trimethyl element group from carbon via silicon to germanium. On the other hand, a slight polarization of the Si-methyl bonds with formation of a positive partial charge on the silicon, which is less pronounced in the germanium compound and therefore more similar to the carbon-containing one. This effect can be explained by the electronegativities: The EN of carbon and germanium are more similar to each other than the EN of Silicon.

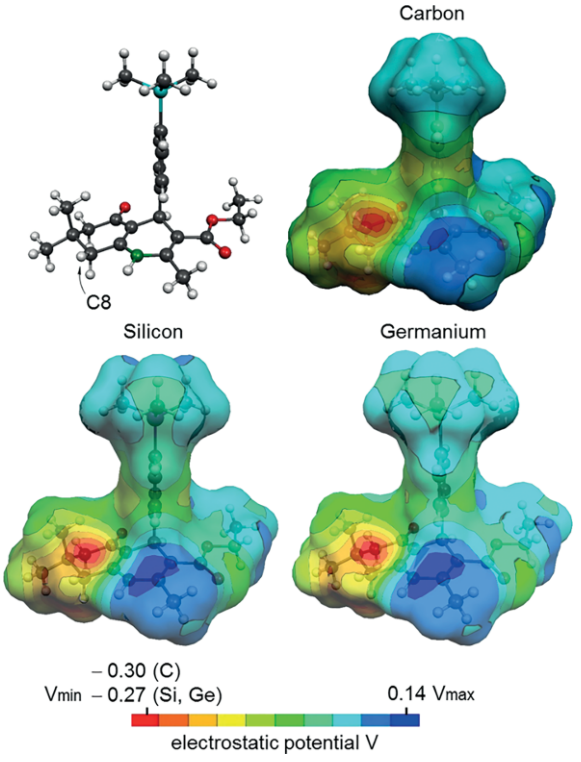

Figure 5. Conolly surfaces (sample radius 1.4 Å), occupied with the electrostatic potential of carbon, silicon and germanium dihydropyridines **2**, **6a**, and **6b** in comparison.

Additionally, this similarity of carbon and germanium was observed in chromatographic experiments. Following usual principles, especially regarding the size of the trimethyl element groups, a development of chromatographic properties from carbon via silicon to germanium could be expected. As Figure 6 reveals, the silicon compound **6a** differs strongly from the carbon and germanium analogues **2** and **6b**, respectively.

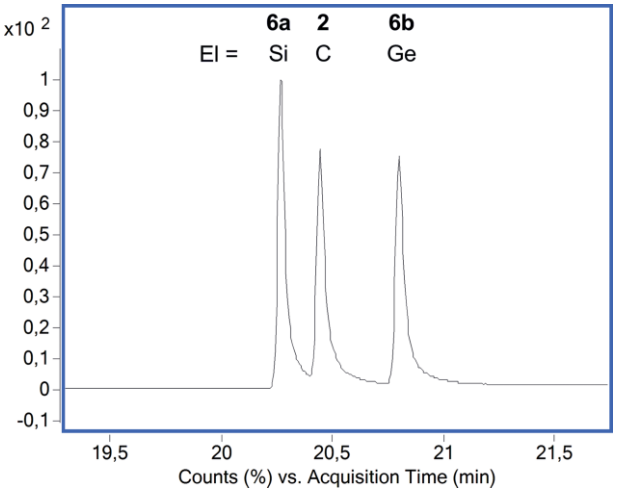

Figure 6. Extract from the gas chromatogram of a mixture of compounds **6a**, **2** and **6b**. Column material: silica, 0.25 mm; eluent: He.

In corresponding HPLC experiments, the same unexpected order of the three compounds is observed (see Supplementary Information for further details).

Additionally, there is one aspect that has already been discovered in our previous studies: a localized, relatively strongly marked negative potential at C8 of the fused ring system.[5] This charge can also be seen on the flat underside of the molecule, as shown in Figure 7. The more electronegative and electron-rich oxygen atoms do not contribute to the development of a negative electrostatic potential because their electrons are delocalized due to mesomerism. Furthermore, it is noticeable that a very strong potential gradient is present on the surface. In the direction of the center of the molecule, the partial charge changes very rapidly from negative to clearly positive values. This positive surface is most pronounced with silicon DHP. This again could be explained by the electronegativities of the elements.

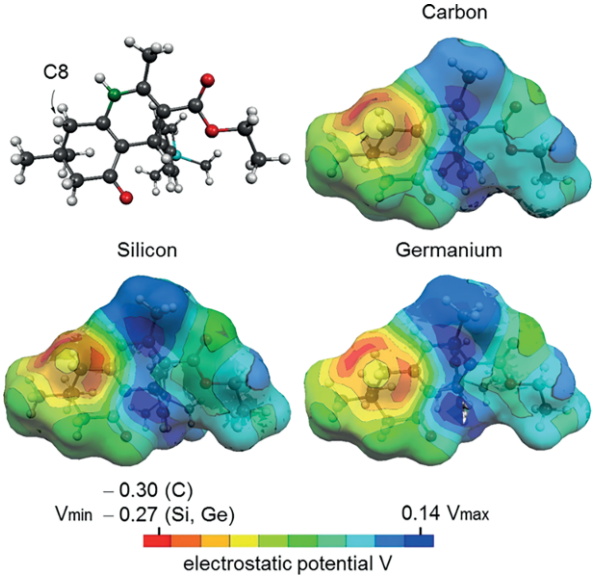

Figure 7. Conolly surfaces (sample radius 1.4 Å), occupied with the electrostatic potential of carbon, silicon and germanium dihydropyridines **6a**, **6b**, and **2** in comparison.

The biological activity of silicon and germanium DHP was tested in a Smad4-binding element (SBE4) reporter gene assay in HEK293T as reported previously (Figure 8).[5] For direct comparison, a potent non-selective ALK4,5,7-inhibitor (SB-431542)[10] and the original DHP **1** were tested. The new silicon (**6a**) and germanium (**6b**) compounds both show almost identical dose-response curves and behave perfectly bioisosteric to their carbon congener as they exhibit the same TGFβ inhibition potency and efficacy, i.e. with an IC_{50} of 0.28 μM and maximum pathway inhibition >95 % (Table 1). With that profile they also outperform the original 4′-Ph-substituted DHP **1**.

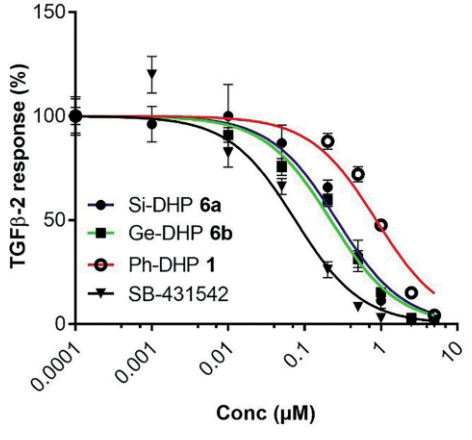

Figure 8. Representative TGFβ inhibition curves of higher carbon containing 1,4-DHPs **6a** and **6b** in comparison to the original DHP **1** and the ALK4,5,7 inhibitor SB-431542. (Smad 4-binding element (SBE4) dual luciferase assay in HEK293T cells).[4,5]

Table 1. TGFβ inhibition profiles (IC_{50} values and maximum inhibition at 5 μM) of 4-substituted, bioisosteric 4′-(*tert*-butyl) DHP derivatives.

Compound[a]	IC_{50} [μM]	E_{max} (% inhibition at 5 μM)[a]
Ph-DHP **1**	0.85 ± 0.30[5]	95 ± 2[5]
C-DHP **2**	0.28 ± 0.12[5]	95 ± 4[5]
Si-DHP **6a**	0.28 ± 0.05	98 ± 1
Ge-DHP **6b**	0.28 ± 0.04	98 ± 1

[a] Data from N = 3–4 independent experiments in a Smad 4-binding element (SBE4) dual luciferase assay in HEK293T cells (mean ± SD, normalized to DMSO = 100 %).[5]

Conclusions

In conclusion, we present the synthesis of Si and Ge analogues **6a** and **6b** of the active TGFβ Inhibitor **2**. The investigation of all three compounds by X-ray analysis showed that, except the element–carbon bond lengths, the differences are due to packing effects, and they are located at molecule areas that are flexible in solution. As the pseudo axial arrangement of the aromatic substituent at 4-positions is steeper for the C and Si analogues (compared to **1**), but not for the Ge compound, this seems to be also a packing effect and no indication for activity. Quantum chemical calculations showed that the carbon and germanium compounds differ less, while the silicon one has a slightly positive charge at the Si-center and more negative ones at the methyl groups than the other compounds. This effect is probably based on the element-specific electronegativities. All three of the molecules show a negatively charged area at C8, which has also been detected in active substances of our previous studies.[5] Importantly, all DHP compounds (**2**, **6a**, **6b**) exhibited the same TGFβ inhibition profile, underlining the possibility for bioisosteric replacement. Since Si bioisosters are typically more lipophilic and at the same time could protect from oxidative metabolism, such analogues might exhibit a beneficial pharmacokinetic profile. The same could hold true for germanium analogues. Interestingly, chromatographic experiments as well as electronic examinations revealed a greater difference of silicon and germanium compared to carbon and germanium. This might have influence on a wide range of bioisosteric replacement considerations, underlining that germanium should not be generally neglected in such processes.

Experimental Section

Materials and Methods: All reactions were performed under an Argon atmosphere in flame-dried Schlenk-type glassware on a vacuum line. The solvents diethyl ether (Et_2O) and tetrahydrofuran (THF) were dried with Na/benzophenone and distilled under argon.

^{1}H-NMR (internal standard $CDCl_3$, C_6D_6), ^{13}C-NMR (internal standard $CDCl_3$, C_6D_6) and ^{29}Si-NMR spectra were recorded on a Bruker DRX 300 MHz at room temperature. The ^{13}C-NMR and ^{29}Si-NMR spectra were recorded ^{1}H-broadband decoupled ({^{1}H}). The ^{29}Si-NMR are referred to TMS as external standard and measured via the INEPT pulse sequence. For the assignment of the multiplicities, the following abbreviations were used: s = singlet, brs = broad singlet, d = doublet, t = triplet, m = multiplet. Data were processed using ACD/NMR Processor Academic Edition (Product Version 12.01).

Single-crystal X-ray diffraction analysis was performed on an Oxford Diffraction Xcalibur S diffractometer using graphite-monochromated Mo-K_α radiation (λ = 0.71073 Å). Determination of the unit cells and data collection was carried out at 100 K. The crystal structure were solved with direct methods (*SHELXS-97*) and refine against F^2 with the full-matrix least-squares method (*SHELXL*-97). A multiscan adsorption correction using the implemented CrysAlis RED program was employed. The non-hydrogen atoms were refined anistropically.

CCDC 1943895 (for **6a**), 1943893 (for **6b**), and 1943894 (for **2**) contain the supplementary crystallographic data for this paper. These data can be obtained free of charge from The Cambridge Crystallographic Data Centre.

Synthetic Procedures:

(4-Bromophenyl)trimethylsilane (4a): To the solution of 1,4-dibrombenzene (1.50 g, 6.36 mmol) in Et_2O (13 mL) *n*BuLi (2.54 mL, 2.50 M, 6.36 mmol) was added dropwise at –78 °C. The reaction mixture was stirred at –78 °C for 4 h. After adding chlorotrimethylsilane (0.76 g, 7.00 mmol) the reaction mixture was slowly warmed to room temperature and stirred overnight at room temperature. Then the reaction mixture was quenched by the addition of H_2O. The aqueous phase was extracted with Et_2O and the combined organic phases were washed with aqueous saturated NaCl solution and dried with Na_2SO_4. After removal of all volatile components the product could be obtained as a colorless, viscous liquid (yield: quantitative). The reaction product was used without further purification in the following synthesis step. ^{1}H-NMR (300 MHz, $CDCl_3$): δ = 0.30 [s, 9H, Si(C*H*$_3$)$_3$], 7.39–7.43 [m, 2H, Si(CH$_3$)$_3$CC*H*], 7.50–7.54 (m, 2H, BrCC*H*) ppm; ^{13}C{^{1}H}-NMR (75 MHz, $CDCl_3$): δ = –1 [3C, Si(*C*H$_3$)$_3$], 124 (1C, Br*C*), 131 (2C, BrCCH), 135 [2C, Si(CH$_3$)$_3$C*C*H], 139 [1C, Si(CH$_3$)$_3$*C*] ppm; ^{29}Si{^{1}H}-NMR (60 MHz, $CDCl_3$): δ = –3.4 ppm; GC/EI-MS [80 °C (1 min) – 300 °C (5.5 min)] t_R = 3.82 min, *m/z* (%): 228 (13) (M^+), 213 (99) [(M – Me)$^+$].

(4-Bromophenyl)trimethylgermane (4b): To the solution of 1,4-dibrombenzene (1.50 g, 6.36 mmol) in Et_2O (13 mL) *n*BuLi (2.54 mL, 2.5 M, 6.36 mmol) was added dropwise at –78 °C. The reaction mixture was stirred at –78 °C for 4 h. After adding chlorotrimethylgermane (1.10 g, 7.00 mmol) the reaction mixture was slowly warmed to room temperature and stirred overnight at room temperature. Then the reaction mixture was quenched by the addition of H_2O. The aqueous phase was extracted with Et_2O and the combined organic phases were washed with aqueous saturated NaCl solution and dried with Na_2SO_4. After removal of all volatile components the product could be obtained as a colorless, viscous liquid (yield: 1.67 g, 6.12 mmol, 96 %). The reaction product was used without further purification in the following synthesis step. ^{1}H-NMR (300 MHz, $CDCl_3$): δ = 0.39 [s, 9H, Ge(C*H*$_3$)$_3$], 7.34 [d, *J*(H,H) = 8.05 Hz, 2H, Ge(CH$_3$)$_3$CC*H*], 7.49 [d, *J*(H,H) = 8.05 Hz, 2H, BrCC*H*] ppm; ^{13}C{^{1}H}-NMR (75 MHz, $CDCl_3$): δ = 2 [3C, Ge(*C*H$_3$)$_3$], 123 (1C, Br*C*), 131 (2C, BrCCH), 135 [2C, Ge(CH$_3$)$_3$C*C*H], 141 [1C, Ge(CH$_3$)$_3$*C*] ppm; GC/EI-MS [80 °C (1 min) – 300 °C (5.5 min)] t_R = 7.71 min, *m/z* (%): 274 (7) (M^+), 259 (100) [(M – Me)$^+$], 229 (12) [(M – 3Me)$^+$].

4-(Trimethylsilyl)benzaldehyde (5a): To a solution of (4-bromophenyl)trimethylsilane (1.50 g, 6.54 mmol) in THF (40 mL) *n*BuLi (2.88 mL, 2.50 M, 7.19 mmol) was added dropwise at –78 °C. The reaction mixture was stirred at –78 °C for 15 min. After adding dimethylformamide (1.43 g, 19.6 mmol), the reaction mixture was slowly warmed to room temperature and stirred overnight at room temperature. Then the reaction mixture was quenched by the addition of aqueous saturated NH_4Cl solution. The aqueous phase was extracted with Et_2O and the combined organic phases were washed with aqueous saturated NaCl solution and dried with Na_2SO_4. After removal of all volatile components and column chromatographic purifying (pentane, pentane/Et_2O = 100:1 → 50:1) the product could be obtained as a colorless, viscous liquid (yield: 0.87 g, 4.88 mmol, 75 %). ^{1}H-NMR (300 MHz, $CDCl_3$): δ = 0.32 [s, 9H, Si(C*H*$_3$)$_3$], 7.70 [d, *J*(H,H) = 8.05 Hz, 2H, Si(CH$_3$)$_3$CC*H*], 7.85 [d, *J*(H,H) = 8.42 Hz, 2H, (HCO)CC*H*], 10.03 (s, 1H, *H*CO) ppm; ^{13}C{^{1}H}-NMR (75 MHz, $CDCl_3$): δ = 1 [3C, Si(*C*H$_3$)$_3$], 129 [2C, (HCO)C*C*H], 134 [2C, Si(CH$_3$)$_3$C*C*H], 136 [1C, (HCO)*C*], 149 [1C, Si(CH$_3$)$_3$*C*], 193 (1C, H*C*O) ppm; ^{29}Si{^{1}H}-NMR (60 MHz, $CDCl_3$): δ = –2.7 ppm; GC/EI-MS [80 °C (1 min) – 300 °C (5.5 min)] t_R = 3.91 min; *m/z* (%): 178 (22) (M^+), 163 (100) [(M – Me)$^+$].

4-(Trimethylgermyl)benzaldehyde (5b): To a solution of (4-bromophenyl)trimethylgermane (1.67 g, 6.12 mmol) in THF (38 mL) *n*BuLi (2.69 mL, 2.50 M, 6.73 mmol) was added dropwise at –78 °C. The reaction mixture was stirred at –78 °C for 15 min. After adding dimethylformamide (1.34 g, 18.4 mmol) the reaction mixture was slowly warmed to room temperature and stirred overnight at room temperature. Then the reaction mixture was quenched by the addition of aqueous saturated NH_4Cl solution. The aqueous phase was extracted with Et_2O and the combined organic phases were washed with aqueous saturated NaCl solution and dried with Na_2SO_4. After removal of all volatile components and column chromatographic purifying (pentane, pentane/Et_2O = 100:1 → 50:1) the product could be obtained as a colorless, viscous liquid (yield: 1.05 g, 4.70 mmol, 77 %). ^{1}H-NMR (300 MHz, $CDCl_3$): δ = 0.44 [s, 9H, Ge(C*H*$_3$)$_3$], 7.66 [d, *J*(H,H) = 8.05 Hz, 2H, Ge(CH$_3$)$_3$CC*H*], 7.84 [d, *J*(H,H) = 8.05 Hz, 2H, (HCO)CC*H*], 10.01 (s, 1H, *H*CO) ppm; ^{13}C{^{1}H}-NMR (75 MHz, $CDCl_3$): δ = –2 [3C, Ge(*C*H$_3$)$_3$], 129 [2C, (HCO)C*C*H], 134 [2C, Ge(CH$_3$)$_3$C*C*H], 136 [1C, (HCO)*C*], 152 [1C, Ge(CH$_3$)$_3$*C*], 193 (1C, H*C*O) ppm; GC/EI-MS [80 °C (1 min) – 300 °C (5.5 min)] t_R = 4.16 min, *m/z* (%): 224 (2) (M^+), 209 (100) [(M – Me)$^+$], 179 (13) [(M – 3Me)$^+$].

General Procedure for the Synthesis of 1,4-dihydropyridine (DHP): To a solution of dimedone, ammonium acetate and acetylacetone in ethanol the benzaldehyde and iodine was added. The reaction mixture was stirred overnight at room temperature. After removal of all volatile components the residue was dissolved in EtOAc. The organic phase was washed with aqueous saturated $Na_2S_2O_3$ and aqueous saturated NaCl solution and dried with Na_2SO_4. After removal of all volatile components the products were purified per individual techniques as noted below.

C-DHP 2: The reaction of dimedone (86.9 mg, 0.62 mmol), ammonium acetate (67.1, 0.87 mmL), acetylacetone (80.7 mg, 0.62 mmol), 4-*tert*-butylbenzaldehyde (100 mg, 0.62 mmol), iodine (45.5 mg, 0.18 mmol) in EtOH (1.24 mL) gave after column chromatographic purification (pentane/Et_2O = 5:1 → 2:1 → 1:1 → 1:2 → 1:5 →1:10) yellowish crystals (yield: 21 mg, 0.053 mmol, 9 %). ^{1}H-NMR (300 MHz, C_6D_6): δ = 0.76 [s, 3H, (CO)CH$_2$CC*H*$_3$], 0.79 [s, 3H, (CO)CH$_2$CC*H*$_3$], 0.93 [t, *J*(H,H) = 6.95 Hz, 3H, OCH$_2$C*H*$_3$], 1.10–1.24 [s, 9H, C(C*H*$_3$)$_3$], 1.88 (s, 2H, NCC*H*$_2$), 2.07 [d, *J*(H,H) = 4.39 Hz, 2H, (CO)C*H*$_2$], 2.35 (s, 3H, NCC*H*$_3$), 3.95 (q, *J*(H,H)= 7.20 Hz, 2H, OC*H*$_2$), 5.64 (s, 1H, C*H*), 6.93 (s, 1H, N*H*), 7.35 [d, *J*(H,H) = 7.68 Hz, 2H,

$C(CH_3)_3CCH_{ortho}$], 7.67 [d, *J*(H,H) = 7.32 Hz, 2H; $C(CH_3)_3CCHCH_{meta}$] ppm; $^{13}C\{^1H\}$-NMR (75 MHz, C_6D_6): δ = 14 (1C, OCH_2CH_3), 19 (1C, $NCCH_3$), 27 [1C, $(CO)CH_2CCH_3$], 29 [1C, $(CO)CH_2CCH_3$], 32 [3C, $C(CH_3)_3$], 33 [1C, $(CO)CH_2C(CH_3)_2$], 34 [1C, $C(CH_3)_3$], 37 [1C, (CO)CCH], 41 (1C, $NCCH_2$), 51 [1C, $(CO)CH_2$], 60 (1C, OCH_2CH_3), 107 [1C, NCC(COOEt)], 112 [1C, NCC(CO)], 125 [2C, $(CH_3)_3CCCH$], 128 [2C, $(CH_3)_3CCCHCH$], 144 [2C, $(CH_3)_3CCCHCHC$], 145 [1C, $(CH_3)_3CC$], 149 (1C, $NCCH_2$), 149 (1C, $NCCH_3$), 168 (1C, COOEt), 196 (1C, CO) ppm; GC-EI/MS [80 °C (1 min) – 300 °C (5.5 min)] t_R = 9.11 min, *m/z* (%): 395 (17) (M^+), 262 (100) [$(M–Me_3CPh)^+$].

Si-DHP 6a: The reaction of dimedone (78.6 mg, 0.56 mmol), ammonium acetate (43.2 mg, 0.56 mmL), acetylacetone (72.9 mg, 0.17 mmol), 4-(trimethylsilyl)benzaldehyde (42.6 mg, 0.56 mmol), iodine (45.5 mg, 0.17 mmol) in EtOH (1.40 mL) gave after column chromatographic purification (pentane/Et_2O = 5:1 → 2:1 → 1:1 → 1:2 → 1:5 →1:10) and recrystallization in EtOH yellowish crystals (yield: 108 mg, 0.26 mmol, 46 %). ^{1}H-NMR (300 MHz, $CDCl_3$): δ = 0.18 [s, 9H, $Si(CH_3)_3$], 0.94 [s, 3H, $(CO)CH_2CCH_3$], 1.05 (s, 3H, (CO)CH2CCH_3), 1.20 (t, *J*(H,H) = 7.14 Hz, 3H, OCH_2CH_3), 2.06–2.42 [m, 7H, $(CO)CH_2$, $NCCH_2$, $NCCH_3$], 4.06 (q, *J* = 6.95 Hz, 2H, OCH_2), 5.02 (s, 1H, CH), 6.80 (br. s., 1H, NH), 7.15–7.50 (m, 4H, $CH_{aromatic}$) ppm; $^{13}C\{^1H\}$-NMR (75 MHz, $CDCl_3$): δ = –1 [3C, $Si(CH_3)_3$], 14 (1C, OCH_2CH_3), 19 (1C, $NCCH_3$), 27 [1C, $(CO)CH_2CCH_3$], 29 [1C, $(CO)CH_2CCH_3$], 33 [1C, $(CO)CH_2C(CH_3)_2$], 37 [1C, (CO)CCH], 41 (1C, $NCCH_2$), 51 [1C, $(CO)CH_2$], 60 (1C, OCH_2CH_3), 106 [1C, NCC(COOEt)], 112 [1C, NCC(CO)], 127 [2C, $(CH_3)_3SiCCH$], 133 [2C, $(CH_3)_3SiCCHCH$], 137 [1C, $(CH_3)_3SiC$], 144 [2C, $(CH_3)_3SiCCHCHC$], 1478 (1C, $NCCH_2$), 149 (1C, $NCCH_3$), 168 (1C, COOEt), 196 (1C, CO) ppm; $^{19}Si\{^1H\}$-NMR (60 MHz, $CDCl_3$): δ = –4.4 (1Si) ppm; GC/EI-MS [80 °C (1 min) – 300 °C (5.5 min)] t_R = 8.95 min, *m/z* (%): 411 (11) (M^+), 262 (100) [$(M–Me_3SiPh)^+$]. elemental analysis calcd. (%) for $C_{24}H_{33}NO_3Si$: C 70.03, H 8.08, N 3.40; found C 69.7, H 8.1, N 3.1.

Ge-DHP 6b: The reaction of dimedone (63.1 mg, 0.45 mmol), ammonium acetate (34.7, 0.45 mmL), acetylacetone (58.6 mg, 0.45 mmol), 4-(trimethylgermyl)benzaldehyde (100 mg, 0.45 mmol), iodine (33.0 mg, 0.13 mmol) in EtOH (1.40 mL) gave after column chromatographic purification (pentane/Et_2O = 5:1 → 2:1 → 1:1 → 1:2 → 1:5 →1:10) and recrystallization in EtOH yellowish crystals (yield: 72.0 mg, 0.16 mmol, 35 %). ^{1}H-NMR (300 MHz, $CDCl_3$): δ = 0.30 [s, 9H, $Ge(CH_3)_3$], 0.94 [s, 3H, $(CO)CH_2CCH_3$], 1.05 (s, 3H; $(CO)CH_2CCH_3$), 1.21 (t, *J* = 7.14 Hz, 3H; OCH_2CH_3), 2.07–2.42 [m, 7H; $(CO)CH_2$, $NCCH_2$, $NCCH_3$], 4.05 („q", *J* = 6.95 Hz, 2H; OCH_2), 5.02 (s, 1H; CH), 6.61 (br. s., 1H; NH) 7.19–7.40 (m, 4 H; $CH_{aromatic}$) ppm; $^{13}C\{^1H\}$-NMR (75 MHz, C_6D_6): δ = –2 [3C, $Ge(CH_3)_3$], 14 (1C, OCH_2CH_3), 19 (1C, $NCCH_3$), 27 [1C, $(CO)CH_2CCH_3$], 29 [1C, $(CO)CH_2CCH_3$], 33 [1C, $(CO)CH_2C(CH_3)_2$], 36 [1C, (CO)CCH], 41 (1C, $NCCH_2$), 51 [1C, $(CO)CH_2$], 60 (1C, OCH_2CH_3), 106 [1C, NCC(COOEt)], 112 [1C, NCC(CO)], 128 [2C, $(CH_3)_3GeCCH$], 133 [2C, $(CH_3)_3GeCCHCH$], 140 [1C, $(CH_3)_3GeC$], 144 [2C, $(CH_3)_3GeCCHCHC$], 147 (1C, $NCCH_2$), 149 (1C, $NCCH_3$), 168 (1, COOEt), 196 (1C, CO) ppm; GC/EI-MS [80 °C (1 min) – 300 °C (5.5 min)] t_R = 9.33 min, *m/z* (%): 457 (4) (M^+), 262 (100) [$(M–Me_3GePh)^+$]. elemental analysis calcd. (%) for $C_{24}H_{33}NO_3Ge$: C 63.19, H 7.29, N 3.07; found C 63.2, H 7.3, N 2.9.

TGFβ/Smad assay: A SMAD-4 binding element (SBE-4)-based transient luciferase reporter gene assay (in 293T cells) was performed as described previously in detail. In brief, cells were batch-transfected with a SBE4-firefly luciferase and TK-driven renilla luciferase plasmid, replated after ca. 12 h on 96-well plates and incubated for 2 hours before addition of compounds, DMSO and TGFβ-2 (10 ng/mL). Each condition was done in triplicate. After overnight incubation, firefly and renilla luciferase activities were quantified on a Tecan Infinite M1000 (Crailsheim, Germany) following the instructions of the DualGlo Assay-Kit (Promega, Madison, USA). GraphPad Prism 5 was used for data evaluation.

Acknowledgments

We thank Stephanie Schulze for her efforts in the HPLC experiments and the Deutsche Forschungsgemeinschaft (DFG) and the Fonds der Chemischen Industrie for financial support.

Keywords: Bioisosters · Silicon · Germanium · 1,4-Dihydropyridines · TGFβ inhibitors

[1] a) C. H. Heldin, K. Miyazono, P. ten Dijke, *Nature* **1997**, *390*, 465–471; b) K. Wharton, R. Derynck, *Development* **2009**, *136*, 3691–3697.
[2] a) J. M. Yingling, K. L. Blanchard, J. S. Sawyer, *Nat. Rev. Drug Discovery* **2004**, *3*, 1011–1022; b) S. Colak, P. Ten Dijke, *Trends Cancer* **2017**, *3*, 56–71.
[3] E. Willems, J. Cabral-Teixeira, D. Schade, W. Cai, P. Reeves, P. J. Bushway, M. Lanier, C. Walsh, T. Kirchhausen, J. C. I. Belmonte, J. Cashman, M. Mercola, *Cell Stem Cell* **2012**, *11*, 242–252.
[4] D. Schade, M. Lanier, E. Willems, K. Okolotowicz, P. Bushway, C. Wahlquist, C. Gilley, M. Mercola, J. R. Cashman, *J. Med. Chem.* **2012**, *55*, 9946–9957.
[5] a) D. Längle, V. Marquardt, E. Heider, B. Vigante, G. Duburs, I. Luntena, D. Flötgen, C. Golz, C. Strohmann, O. Koch, D. Schade, *Eur. J. Med. Chem.* **2015**, *95*, 249–266; b) D. Längle, T. R. Werner, F. Wesseler, E. Reckzeh, N. Schaumann, L. Drowley, M. Polla, A. T. Plowright, M. N. Hirt, T. Eschenhagen, D. Schade, *ChemMedChem* **2019**, *14*, 1–14.
[6] See ref.[4]
[7] a) N. R. Perestelo, G. G. Llanos, C. P. Reyes, A. Amesty, K. Sooda, S. Afshinjavid, I. A. Jiménez, F. Javid, I. L. Bazzocchi, *J. Med. Chem.* **2019**, *62*, 4571–4585; b) E. Eryilmaz, *Eur. J. Pharm. Sci.* **2019**, *134*, 266–273; c) M. F. Khan, L. Zepeda-Velazquez, M. A. Brook, *Colloids Surf. B* **2015**, *132*, 216–224; d) S. Fujii, Y. Hashimoto, *Future Med. Chem.* **2017**, *9*, 485–202; e) R. Ramesh, D. S. Reddy, *J. Med. Chem.* **2018**, *61*, 3779–3798.
[8] a) B. Célariès, M. Gielen, D. de Vos, G. Rima, *Appl. Organomet. Chem.* **2003**, *17*, 191–193; b) S. Fujii, Y. Miyajima, H. Masuno, H. Kagechika, *J. Med. Chem.* **2013**, *56*, 160–166; c) E. Lukevics, L. Ignatovich, *Appl. Organomet. Chem.* **1992**, *6*, 113–126; d) E. Lukevics, L. Ignatovich, I. Shestakova, *Appl. Organomet. Chem.* **2003**, *17*, 898–905; e) P. G. R. Ortega, M. Montejo, J. J. L. González, *J. Mol. Model.* **2014**, *20*, 2430; f) R. Tacke, T. Heinrich, T. Kornek, M. Merget, S. A. Wagner, J. Gross, C. Keim, G. Lambrecht, E. Mutschler, T. Beckerss, M. Bernd, T. Reissmann, *Phosphorus Sulfur Silicon Relat. Elem.* **1999**, *150*, 69–87; g) T. Yamakawa, H. Kagechika, E. Kawachi, Y. Hashimoto, K. Shudo, *J. Med. Chem.* **1990**, *33*, 1430–1437; h) R. Tacke, D. Reichel, P. G. Jones, X. Hou, M. Waelbroeck, J. Gross, E. Mutschler, G. Lambrecht, *J. Organomet. Chem.* **1996**, *521*, 305–323; i) R. Tacke, M. Merget, R. Bertermann, M. Bernd, T. Beckers, T. Reissmann, *Organometallics* **2000**, *19*, 3486–3497; j) R. Tacke, B. Becker, D. Berg, W. Brandes, S. Dutzmann, S. Schaller, *J. Organomet. Chem.* **1992**, *438*, 45–55.
[9] a) A. F. Hollemann, E. Wiberg, N. Wiberg in *Anorganische Chemie, Vol. 103*, De Gruyter, Berlin, **2017**, p. 1551; b) K. M. Baines, W. G. Stibbs, *Coord. Chem. Rev.* **1995**, *145*, 157–200.
[10] G. J. Inman, F. J. Nicolas, J. F. Callahan, J. D. Harling, L. M. Gaster, A. D. Reith, N. J. Laping, C. S. Hill, *Mol. Pharmacol.* **2002**, *62*, 65–74.

Received: November 13, 2019